

Study on the observation of Eu^{2+} and Eu^{3+} valence states in low silica calcium aluminosilicate glasses

This article has been downloaded from IOPscience. Please scroll down to see the full text article.

2010 J. Phys.: Condens. Matter 22 055601

(<http://iopscience.iop.org/0953-8984/22/5/055601>)

View [the table of contents for this issue](#), or go to the [journal homepage](#) for more

Download details:

IP Address: 129.252.86.83

The article was downloaded on 30/05/2010 at 07:02

Please note that [terms and conditions apply](#).

Study on the observation of Eu^{2+} and Eu^{3+} valence states in low silica calcium aluminosilicate glasses

J A Sampaio¹, M C Filadelpho¹, A A Andrade¹, J H Rohling²,
A N Medina², A C Bento², L M da Silva³, F C G Gandra³,
L A O Nunes⁴ and M L Baesso²

¹ Laboratório de Ciências Físicas, Universidade Estadual do Norte Fluminense, Avenida Alberto Lamego 2000, CEP 28013-600, Campos dos Goytacazes, RJ, Brazil

² Departamento de Física, Universidade Estadual de Maringá, Avenida Colombo 5790, CEP 87020-900, Maringá, PR, Brazil

³ Instituto de Física Gleb Wataghin, Universidade Estadual de Campinas, CEP 13083-970, Campinas, SP, Brazil

⁴ Instituto de Física de São Carlos, Grupo de Espectroscopia de Sólidos, Universidade de São Paulo—USP, CEP 13560-970, São Carlos, SP, Brazil

E-mail: jsampaio@uenf.br

Received 19 October 2009, in final form 1 December 2009

Published 15 January 2010

Online at stacks.iop.org/JPhysCM/22/055601

Abstract

The optical, magnetic and structural properties of Eu doped low silica calcium aluminosilicate glasses were investigated. The optical absorption coefficient presented two bands at 39 246 and 29 416 cm^{-1} , which were assigned respectively to the $4f^7 (^8S_{7/2}) \rightarrow 4f^6 (4F_J) 5d (T_{2g})$, and $4f^7 (^8S_{7/2}) \rightarrow 4f^6 (4F_J) 5d (E_g)$ transitions of Eu^{2+} . The fluorescence measured at 300 K on a sample doped with 0.5 wt% of Eu_2O_3 exhibited a broad band centered at 17 350 cm^{-1} , which is attributed to the $4f^6 5d \rightarrow 4f^7$ transition of Eu^{2+} , whereas the additional peaks are due to the $^5D_0 \rightarrow ^7F_J$ ($J = 1, 2, 4$) transitions of Eu^{3+} . From magnetization and XANES data it was possible to evaluate the fractions of Eu^{2+} and Eu^{3+} for the sample doped with 0.5 and 5.0 wt% of Eu_2O_3 , the values of which were approximately 30 and 70%, respectively.

(Some figures in this article are in colour only in the electronic version)

1. Introduction

Europium doped glasses belong to an important class of materials because they can be employed in a variety of applications such as two-dimensional x-ray imaging sensors, high-density memory devices, blue emitting phosphors for plasma display panels, and x-ray storage [1, 2]. Divalent europium doped materials find applications as luminescent sources in the UV to blue-green region of the electromagnetic spectrum, as well as sensor devices, because the divalent Eu emission intensity is strongly dependent on the temperature [3]. On the other hand, the trivalent Eu doped materials present optical properties of interest in the orange-red region. The advantage of using glasses as hosts for such dopants in relation to crystals lies in their homogeneity and

ease of fabrication into various shapes, such as flat boards, fibers, and rods.

Among the lanthanide elements only Sm, Eu, Tm, and Yb are susceptible to exist in the divalent state [4], and according to Pátek [5], divalent rare earth (RE) ions are an exception in oxide glasses, and only Eu^{2+} can be added into the glass network without difficulty and in a higher fraction than Eu^{3+} ions. The europium divalent state is usually obtained when the frits are melted under a strong reducing atmosphere [6]. In addition, a large part of the trivalent europium ions can be photoreduced permanently to the Eu^{2+} state by femtosecond laser irradiation [7]. In this case, the Eu^{3+} ions at sites with a high covalent degree can be more easily reduced than those at sites with a lower covalence degree. It was shown [8, 9] that depending on the composition and preparation method, the

ratio $\text{Eu}^{3+}/\text{Eu}^{2+}$ can vary from 30 to 100%, as for example in the case of some borate glasses. Whereas in fluorophosphate glasses 30% of Eu ions can be reduced to the Eu^{2+} state, in metaphosphate glasses the proportion is only 2%, and in ultraphosphate glasses there is no observation of such a state.

To the best of our knowledge, investigations regarding Eu in low silica calcium aluminosilicate (LSCA) glasses is very scarce. Actually, only one paper dealing with this subject was reported [10], and only a few of the RE atoms (Nd, Er, Yb, Tb, and Tm) have been studied as dopants in this glass system so far being incorporated into the glass network in the trivalent state [11–16]. The lack of interest in LSCA glasses as RE hosts can be attributed to the crystallization that these elements trigger when the melts are cooled down. Hafner *et al* [17] suggested that studies using neodymium oxide should be abandoned in aluminate glasses because they induce devitrification. However, Sampaio [18] claimed recently that by using standard melting procedures, the amount of RE to be added to the LSCA glass compositions is limited to 8 wt% (~ 2 mol%) Nd_2O_3 , beyond which crystallization takes place. In fact, due to the difficulties in obtaining doped rare earth glasses in this system, the first paper [19] reporting the subject only came out in 1976, seventy seven years after Shepherd *et al* [20] observed that glass could be obtained from non-traditional glass formers, i.e., CaO and Al_2O_3 . In 1978 Davy [21] reported a method of obtaining calcium aluminate glasses with a transparency similar to sapphire, ranging from 0.25 to 6 μm . However, the interest in LSCA glasses as RE hosts has resurged only in the last decade, and since then several works [11–16, 22–27] have reported the thermal, optical, mechanical and spectroscopic properties of such RE doped glasses. Recently [12, 22, 23, 27] LSCA glasses appeared as candidates for solid state laser media hosts because of their good optical and thermo-mechanical properties compared to fluoride, phosphates and silicate glasses [23].

In order to fill in the lack of information regarding Eu in LSCA glasses we investigated their optical, magnetic and structural properties. In addition a comparison between the magnetization and XANES method to evaluate valence states in glasses is carried out.

2. Experiment

The samples with nominal composition 47.4 CaO, 41.5 – x Al_2O_3 , 4.1 MgO, 7.0 SiO_2 , $x = 0, 0.5,$ and 5.0 of Eu_2O_3 (in wt%) were prepared. The reagent grade powders CaCO_3 (99%), Al_2O_3 (99.1%), SiO_2 (99%), MgO (97%) and Eu_2O_3 (99.99%), in 6 g quantities were mixed in a ball mill for 12 h. Afterwards the batches were melted below 1500 °C, under vacuum conditions (10^{-3} mbar) in graphite crucibles, for 2 h for fining. The quenching was made by switching off the heater and moving the crucible up to a cooled vacuum chamber. The annealing was performed by returning the crucible to the melting position, where the temperature was around 900 °C, and allowing it cool down to room temperature. The samples were examined for evidence of crystallinity by x-ray diffraction. Afterwards, they were cut by a slow speed saw into a plate shape, 3 mm \times 3 mm \times 10 mm, and polished

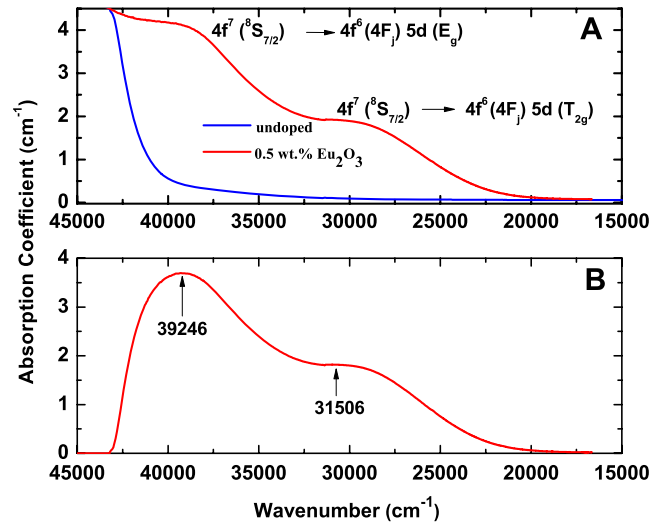


Figure 1. (A) Optical absorption spectra of undoped and 0.5 wt% Eu_2O_3 doped LSCA glasses. (B) Optical absorption coefficient of the 0.5 wt% Eu_2O_3 doped sample obtained by subtracting the contribution of the undoped sample.

optically. The optical absorption spectra were obtained using a spectrophotometer (Perkin Elmer Lambda 900). The photoluminescence measurements were carried out using a monochromator (Spex model 1403), and a photomultiplier (RCA model 31 034) performed at 300 K, and the samples were excited by an Ar laser operating at 333.6 and 363.8 nm. The magnetization (M) measurements were performed using a SQUID facility, in a 2 kOe dc magnetic field. In order to eliminate impurity contributions to the magnetization signal, a magnetization measurement of an undoped sample was also carried out, the data of which was used to subtract from the doped samples magnetization data. Eu L_{III} edge (6977 eV) x-ray absorption spectra were acquired at the LNLS facility in Campinas, Brazil on the D04B-XAFS2 station. The LNLS storage ring is a third-generation synchrotron x-ray source, which operates at 1.37 GeV with a nominal ring current of 250 mA. A Si(111) double-crystal monochromator was used. The XANES (x-ray absorption near-edge structure) spectra were collected in the fluorescence mode, using a 15 element LGe array Canberra GL0055S detector. At least six scans were collected for each sample, which were averaged to increase the quality of the experimental data.

3. Results and discussion

The Eu doped LSCA glass samples prepared under vacuum had an orange-brownish color, which is due to the visible light absorption of the $5d \rightarrow 4f$ transitions of Eu^{2+} . Figure 1(A) shows the optical absorption spectra of the undoped sample, that presented to be nearly constant with wavelength, and of the 0.5 wt% of Eu_2O_3 doped sample, which had two broad absorption edges in the ultraviolet region. This broadness indicates that europium ions interact much more strongly with the glass crystal field compared to other RE ions (Er, Nd, Yb, and Tm) that present sharp absorption lines when

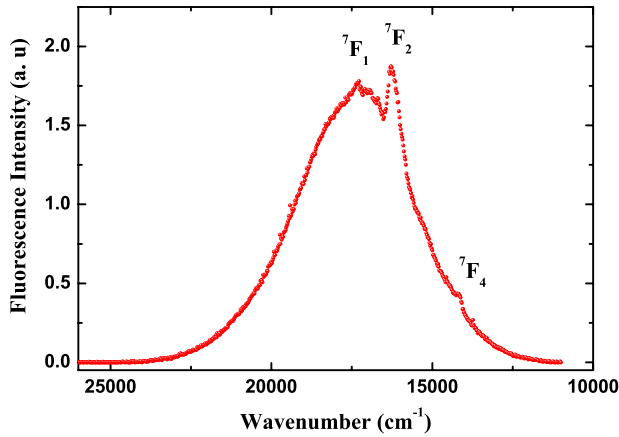


Figure 2. Fluorescence spectrum for a 0.5 wt% Eu_2O_3 doped LSCA glass measured at 300 K. The excitation Ar laser wavelength ranged between 29 976 and 27 487 cm^{-1} .

introduced into the LSCA glass network. The first band, around 39 246 cm^{-1} , can be assigned to the $4f^7 (^8S_{7/2}) \rightarrow 4f^6 (4F_J) 5d (T_{2g})$ transition and the second one, around 31 506 cm^{-1} , to the $4f^7 (^8S_{7/2}) \rightarrow 4f^6 (4F_J) 5d (E_g)$ transition. The absorption in the energies above 40 000 cm^{-1} is associated with the host composition of LSCA glass. Figure 1(B) shows the Eu optical absorption spectrum of a sample doped with 0.5 wt% of Eu_2O_3 obtained by subtracting the contribution of the undoped sample.

Figure 2 shows the absorption and fluorescence spectrum obtained at 300 K for a sample doped with 0.5 wt% of Eu_2O_3 . An overlapping of the broad fluorescence band of Eu^{2+} can be noted, centered at 17 350 cm^{-1} , which is assigned to the allowed $4f^6 5d \rightarrow 4f^7$ transition of the Eu ion, as well as the characteristic sharp lines of Eu^{3+} . These bands correspond to the $^5D_0 \rightarrow ^7F_J$ ($J = 1, 2, 4$) transitions of the trivalent europium, which occurs at 17 303, 16 288, and 14 198 cm^{-1} . The f-f transition of the fluorescence $^5D_0 \rightarrow ^7F_0$, not allowed in the Judd-Ofelt (JO) theory approximation, commonly observed in silicate, borate and fluorophosphate glasses is not presented in Eu doped LSCA glasses. One can observe that the induced dipole transition $^5D_0 \rightarrow ^7F_4$ allowed in JO theory is very weak if compared to the 7F_1 and 7F_2 ones. A reasonable assessment of the splitting magnitude of these transitions levels is difficult to make. First because of the fluorescence band broadness and the smallness of the peaks, secondly because the fluorescence spectrum contains simultaneous contributions of both ions, Eu^{2+} and Eu^{3+} . Accordingly to Nogami *et al* [28], in the co-existence of Eu^{2+} and Eu^{3+} ions, the excited Eu^{2+} in the $4f^6 5d (E_g)$ level decays nonradiatively to the ground state $^8S_{7/2}$, this energy is then transferred to the 7F_0 state of the Eu^{3+} ion that, in turn, is excited to its 5D_2 energy level, eventually decaying from the 5D_0 state to the 7F_0 one as fluorescence, which explains the additional peaks observed. To better understand the fluorescence processes involved in this Eu doped glass system, a systematic study on doping concentration, and time-resolved fluorescence spectroscopy as a function of temperature is being carried out.

The $\text{Eu}^{2+}/\text{Eu}^{3+}$ ratio was obtained from magnetization measurements as follow: at high temperatures (>200 K), the

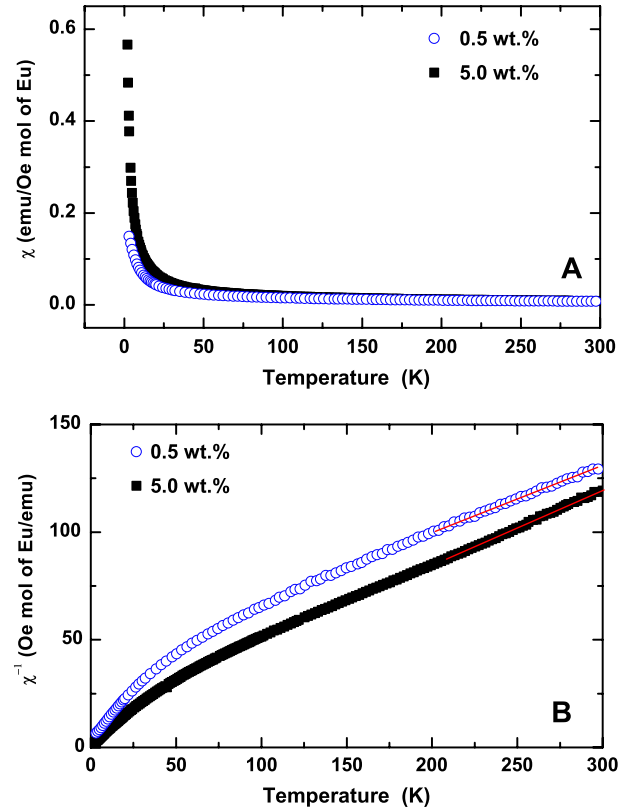


Figure 3. (A) Magnetization and (B) reciprocal magnetic susceptibility as a function of temperature, measured on 0.5 and 5.0 wt% Eu_2O_3 doped LSCA glasses, both measured in a dc magnetic field of 2 kOe.

Eu magnetic susceptibility, χ , can be represented by the Curie-Weiss law given by [29]:

$$\chi = \frac{N_a p^2 \mu_B^2}{3k_B(T - \theta)} = \frac{C}{(T - \theta)}, \quad (1)$$

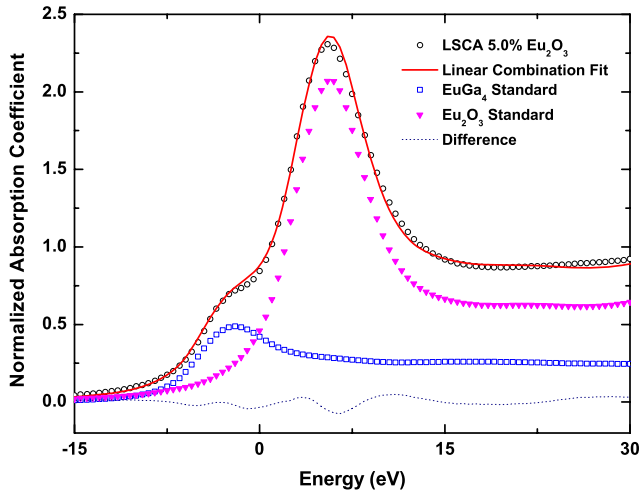
where N_a is the Avogadro number, μ_B is the Bohr magneton, k_B is the Boltzmann constant, T is the temperature, θ is the Curie-Weiss parameter, p is the effective magnetic moment, and $C = N_a p^2 \mu_B^2 / 3k_B$ is the Curie constant.

$$\chi^{-1} = \left(-\frac{\theta}{C}\right) + \left(\frac{1}{C}\right)T = A + BT. \quad (2)$$

The magnetic susceptibility as a function of temperature for the 0.5 and 5.0 wt% Eu_2O_3 doped samples is depicted in figure 3(A), whereas the reciprocal magnetic susceptibility, $\chi^{-1} = H/M$ (given in Oe mol of Eu/emu), is shown in figure 3(B). Taking into account only the high temperature range, from 200 up to 300 K, of the reciprocal magnetic susceptibility and using equation (2) to fit the data, one can obtain the parameters $C = 3.26 \pm 0.03$ K emu mol $^{-1}$ Oe $^{-1}$ and $\theta = -127 \pm 9$ K, and $C = 2.82 \pm 0.02$ K emu mol $^{-1}$ Oe $^{-1}$ and $\theta = -40 \pm 5$ K, respectively for the samples doped with 0.5 and 5.0 wt% Eu_2O_3 . Thus, the calculation of the effective magnetic moment is straightforward, in this case, $p = 5.1$ and 4.8, respectively. The effective magnetic moment for Eu^{3+} is 3.4 μ_B and the theoretical free-ion effective magnetic

Table 1. Magnetization and XANES data (Note: C units in $(\text{K emu mol}^{-1} \text{Oe}^{-1})$.)

Wt% of Eu_2O_3 in the sample	C	θ (K)	p	Obtained from magnetization data		Obtained from XANES spectra	
				Amount of Eu^{2+} (%)	Amount of Eu^{3+} (%)	Amount of Eu^{2+} (%)	Amount of Eu^{3+} (%)
0.5	36.0 ± 0.6	-127 ± 9	5.1	37 ± 3	63 ± 3	24.4 ± 0.3	75.6 ± 0.3
5.0	14.0 ± 0.4	-40 ± 5	4.8	30 ± 3	70 ± 3	26.2 ± 0.4	73.8 ± 0.4

**Figure 4.** XANES spectra of the Eu L_{III} edge for pure Eu_2O_3 , Eu_2Ga_4 and for a 5.0 wt% Eu_2O_3 doped LSCA glass.

moment for Eu^{2+} is $8 \mu_{\text{B}}$ [29]. Using a linear equation such as $\mu_{\text{B}}^{\text{Eu}^{2+}} x - \mu_{\text{B}}^{\text{Eu}^{3+}} (1 - x) = p$, where x is the relative quantity of Eu^{2+} , we can obtain the amount (in percentage) of Eu^{3+} and Eu^{2+} . For the sample doped with 0.5 wt% of Eu_2O_3 the amount of Eu^{2+} was $(37 \pm 3)\%$ and of Eu^{3+} was $(63 \pm 3)\%$; in the case of the sample doped with 5.0 wt% of Eu_2O_3 the values obtained were $(30 \pm 3)\%$ of Eu^{2+} and $(70 \pm 3)\%$ of Eu^{3+} .

Figure 4 shows the x-ray normalized absorption coefficient as a function of energy, in the XANES region, of a LSCA sample doped with 5.0 wt% of Eu_2O_3 . One can observe from this spectrum a double peaked structure, with a peak separation of about 8 eV, which is characteristic of a mixed-valent state of Eu. The low energy peak is assigned to the $4f^7(5d6s)^2$ electronic configuration of Eu, whereas the high energy peak is a fingerprint of its $4f^6(5d6s)^3$ configuration [30]. The valence states were obtained by performing the linear combination fitting of this curve and the spectra from the intensities of the two corresponding white lines of standards, i.e., EuGa_4 where Eu is known to be in the divalent state [31], and Eu_2O_3 for Eu^{3+} state. From the fitting performed using Athena software (IFEFIT package) [32], it was found for a LSCA glass sample doped with 0.5 wt% Eu_2O_3 that the amount of divalent Eu is $(24.4 \pm 0.3)\%$ and of trivalent Eu is $(75.6 \pm 0.3)\%$. Following the same procedure, the values obtained for the sample doped with 5.0 wt% Eu_2O_3 were $(26.2 \pm 0.4)\%$ and $(73.8 \pm 0.4)\%$, respectively for Eu^{2+} and Eu^{3+} . Table 1 summarizes the Eu values of the valence states obtained using both techniques, magnetization and XANES. It is worth noting that the valence states obtained by magnetization measurements had greater values than those obtained by XANES, mainly for the less

doped sample, where the difference, by comparing both results, is about 13% of the overall amount of Eu. This difference can be attributed to the sensitivity of both techniques, since magnetization measurements for very diluted doping have a lower magnetization signal. In addition, in the data analysis the effect of the crystal field at high temperature on the magnetization data was not taken into account. By doing so, any contribution of the crystal field to the orbital magnetic moments is neglected, thus this issue could also explain differences between magnetic measurements and XANES data. However XANES spectroscopy is much more sensitive, because it probes the ion itself, being very sensitive to low diluted impurities in the amorphous system.

4. Conclusion

In this work optical, magnetization and XANES data were used to evaluate the Eu valence state in doped Eu_2O_3 LSCA glasses prepared under vacuum conditions. According to magnetization analysis the amount of Eu^{2+} and Eu^{3+} ions was about 30 and 70% respectively, whereas XANES analysis provided similar results, nevertheless the amount of Eu^{2+} ions present in the samples according to this analysis was at least 5% smaller. However, for very dilute doping concentration the XANES analysis proved to be easier and more accurate. These results indicate that LSCA glasses are promising materials for use in photonic devices.

Acknowledgments

This work was supported under the auspices of the Brazilian agencies CNPq, CAPES and FAPERJ, and FAPESP. We are very grateful to the Brazilian Synchrotron Light Laboratory (LNLS) for their support in XANES experiments carried out at D04B-XAFS2 line (proposal 6594).

References

- [1] Aitasalo T, Deren P, Holsa J, Jungner H, Krupa J C, Lastusaari M, Legendziewicz J, Niittykoski J and Strek W 2003 Persistent luminescence phenomena in materials doped with rare earth ions *J. Solid State Chem.* **171** 114–22
- [2] Qiu J, Miura K, Sugimoto N and Hirao K 1997 Preparation and fluorescence properties of fluoroaluminate glasses containing Eu^{2+} ions *J. Non-Cryst. Solids* **213/214** 266–70
- [3] Shelby J E (ed) 1994 *Rare Elements in Glasses (Key Engineering Materials)* vol 94/95 (Zurich: Trans Tech Publications)

- [4] Flahaut J 1969 *Les Éléments des Terres Rares* (Paris: Masson et Cie Éditeurs)
- [5] Pátek K 1970 *Glass Lasers* (London: Iliffe Books)
- [6] Poort S H M, Reijnhoudt H M, van der Kuip H O T and Blasse G 1996 Luminescence of Eu^{2+} in silicate host lattices with alkaline earth ions in a row *J. Alloys Compounds* **241** 75–81
- [7] Qiu J, Kojima K, Miura K, Mitsuyu T and Hirao K 1999 Infrared femtosecond laser pulse-induced permanent reduction of Eu^{3+} to Eu^{2+} in fluorozirconate glasses *Opt. Lett.* **24** 786–8
- [8] Ebdorff-Heidepriem H and Ehrt D 2000 Formation and UV absorption of cerium, europium and terbium ions in different valencies in glasses *Opt. Mater.* **15** 7–25
- [9] Tanaka K, Fujita K, Soga N, Qiu J and Hirao K 1997 Faraday effect of sodium borate glasses containing divalent europium ions *J. Appl. Phys.* **82** 840–4
- [10] Andrade A A, Coutinho M F, de Castro M P P, Vargas H, Rohling J H, Novatski A, Astrath N G C, Pereira J R D, Bento A C, Baesso M L, Oliveira S L and Nunes L A O 2006 Luminescence quantum efficiency investigation of low silica calcium aluminosilicate glasses doped with Eu_2O_3 by thermal lens spectrometry *J. Non-Cryst. Solids* **352** 3624–7
- [11] Oliveira S L, Lima S M, Catunda T, Vargas H, Nunes L A O, Rohling J H, Bento A C and Baesso M L 2005 Thermal lens determination of fluorescence quantum efficiency of $\text{F}_{3/4}$ level of Tm^{3+} ions in solids *J. Physique IV* **125** 193–6
- [12] Sampaio J A, Gama S, Baesso M L and Catunda T 2005 Fluorescence quantum efficiency of Er^{3+} in low silica calcium aluminate glasses determined by mode-mismatched thermal lens spectrometry *J. Non-Cryst. Solids* **351** 1594–602
- [13] de Sousa D F, Sampaio J A, Nunes L A O, Baesso M L, Bento A C and Miranda L C M 2000 Energy transfer and the $2.8 \mu\text{m}$ emission of Er^{3+} and Yb^{3+} doped low silica content calcium aluminate glasses *Phys. Rev. B* **62** 3176
- [14] Chung W J and Heo J 2001 Energy transfer process for the blue up-conversion in calcium aluminate glasses doped with Tm^{3+} and Nd^{3+} *J. Am. Ceram. Soc.* **84** 348–52
- [15] Hosono H, Kinoshita T, Kawazoe H, Yamazaki M, Yamamoto Y and Sawanobori N 1998 Long lasting phosphorecence properties of Tb^{3+} activated reduced calcium aluminate glasses *J. Phys.: Condens. Matter* **10** 9541–7
- [16] Uhlmann E V, Weinberg M C, Kreidl N J, Burgner L L, Zaroni R and Church K H 1994 Spectroscopic properties of rare-earth-doped calcium-aluminate-based glasses *J. Non-Cryst. Solids* **178** 15–22
- [17] Hafner H C, Kreidl N J and Weidl R A 1958 Optical and physical properties of some calcium aluminate glasses *J. Am. Ceram. Soc.* **44** 315
- [18] Sampaio J A 2001 Synthesis and characterization of low silica calcium aluminosilicate glasses doped with Nd_2O_3 and Er_2O_3 *PhD Thesis* São Paulo State University, Brazil, Oct. 2001
- [19] Jacobs R R and Weber M J 1976 Dependence of the $^4\text{F}_{3/2} \rightarrow ^4\text{I}_{11/2}$ induced-emission cross section for Nd^{3+} on glass composition *IEEE J. Quantum. Electron.* **12** 102–11
- [20] Shepherd E S, Rankin G A and Wright F E 1909 The binary systems of alumina with silica, lime and magnesia *Am. J. Sci.* **28** 293–333
- [21] Davy J R 1978 Development of calcium aluminate glasses for use in infrared-spectrum to $5 \mu\text{m}$ *Glass Technol.* **19** 32–6
- [22] Sampaio J A, Catunda T, Coelho A A, Gama S, Bento A C, Miranda L C M and Baesso M L 2000 Thermo-mechanical and optical properties of calcium aluminosilicate glasses doped with Er^{3+} and Yb^{3+} *J. Non-Cryst. Solids* **273** 239–45
- [23] Sampaio J A, Baesso M L, Gama S, Coelho A A, Eiras J A and Santos I A 2002 Rare earth doping effect on the elastic moduli of low silica calcium aluminosilicate glasses *J. Non-Cryst. Solids* **304** 293–8
- [24] Sampaio J A and Gama S 2004 EXAFS investigation of local structure of Er^{3+} and Yb^{3+} in low silica calcium aluminate glasses *Phys. Rev. B* **69** 10423
- [25] Zou X and Izumitani T 1993 Spectroscopic properties and mechanisms of excited-state absorption and energy-transfer up-conversion for Er^{3+} doped glasses *J. Non-Cryst. Solids* **162** 68–80
- [26] Baesso M L, Bento A C, Andrade A A, Sampaio J A, Pecoraro E, Nunes L A O, Catunda T and Gama S 1998 Absolute thermal lens method to determine fluorescence quantum efficiency and concentration quenching of solids absolute thermal lens method to determine fluorescence quantum efficiency and concentration quenching of solids *Phys. Rev. B* **57** 10545
- [27] Baesso M L, Bento A C, Duarte A R, Neto A M, Miranda L C M, Sampaio J A, Catunda T, Gama S and Gandra F C G 1999 Nd_2O_3 doped low silica calcium aluminosilicate glasses: thermomechanical properties *J. Appl. Phys.* **85** 8112
- [28] Nogami M, Yamazaki T and Abe Y 1998 Fluorescence properties of Eu^{3+} and Eu^{2+} in $\text{Al}_2\text{O}_3\text{-SiO}_2$ glass *J. Lumin.* **78** 63–8
- [29] Kittel C 2005 *Introduction to Solid State Physics* (New York: Wiley)
- [30] Malterre D, Siari A, Durand J, Krill G and Marchal G 1986 X-ray absorption spectroscopy on amorphous mixed-valent alloys *J. Physique* **2** 991–5
- [31] Bobev S, Bauer E D, Thompson J D and Sarrao J L 2004 Single crystal growth, and magnetic and electronic properties of EuGa_4 *J. Magn. Magn. Mater.* **277** 236–43
- [32] Ravel B and Newville M 2005 ATHENA, ARTEMIS, HEPHAESTUS: data analysis for x-ray absorption spectroscopy using IFEFFIT *J. Synchrotron Radiat.* **12** 537–41